

Initial 3C-2D surface seismic and walkaway VSP results from the 2015 Brooks SuperCable experiment

Kevin W. Hall, J. Helen Isaac, Joe Wong, Kevin L. Bertram, Malcolm B. Bertram, Donald C. Lawton, Xuewei Bao¹, and David W.S. Eaton¹

ABSTRACT

A 3C walkaway VSP and surface seismic experiment was conducted at the Containment and Monitoring Institute (CaMI) Field Research Station (FRS) in May of 2015. Two parallel NE-SW receiver lines were laid out with one line centered on well CMCRI COUNTESS 10-22-17-16, and the other offset 100 m to the northwest. Both receiver lines had single-component SM-24 geophones at a 10 m receiver spacing. In addition, the receiver line centered on the well had three-component SM-7 geophones at a 30 m receiver spacing. A three-component ESG SuperCable was deployed within the well at three different levels, giving receiver positions in the well from 106 to 496 meters depth at a 15 m spacing.

Two source lines (Lines 2014 and 208) were acquired three times, once for each tool position in the well. The source was an IVI EnviroVibe sweeping from 10-200 Hz over 16 s. The NE-SW source line had a Vibe Point (VP) every 10 m, offset to the NW of the surface receiver locations, for a walkaway VSP. A semi-circular source line with a radius of 400 m and a VP every five degrees was acquired for a velocity tomography study. Finally, the NE-SW source line was re-acquired using a variety of m-sequence sweeps as the SuperCable was removed from the well. This report presents a first look at the data and some early results.

INTRODUCTION

A 3C walkaway VSP and surface seismic experiment was conducted at the Containment and Monitoring Institute (CaMI) Field Research Station (FRS) in May of 2015. Two parallel NE-SW receiver lines were laid out with one line (Line 108) centered on well CMCRI COUNTESS 10-22-17-16, and the other (Line 106) offset 100 m to the northwest (Figure 1). Receiver lines 106 and 108 had single-component SM-24 geophones at a 10 m receiver spacing, which were attached to out Aries SPML recorder powered by a diesel generator. In addition, receiver line 108 had three-component SM-7 geophones in nail-type casings at a 30 m receiver spacing. Each SM-7 geophone was attached to a Hawk nodal recorder. A three-component ESG SuperCable was deployed in the well at three different levels, giving receiver positions in the well from 106 to 496 meters depth at a 15 m spacing. These data were recorded using ESG Paladin recorders powered by a gas generator. A Geode recorder was present in the cab of the EnviroVibe in order to record auxiliary traces from the Pelton decoder that is in the Vibe. Unfortunately, these data have highlighted some issues with the Vibe during this survey (Appendix A).

¹ Microseismic Industry Consortium

Two source lines were acquired three times, once for each tool position in the well. The source was an IVI EnviroVibe sweeping from 10-200 Hz linearly over 16 s with an additional 4 s listening time. Source line 208 (NE-SW) had a Vibe Point (VP) every 10 m, offset to the NW of the surface receiver locations, for a walkaway VSP. A semi-circular source line (204) with a radius of 400 m and a VP every five degrees was acquired for a velocity tomography study. Finally, line 208 was re-acquired using a variety of filtered and unfiltered m-sequence sweeps as the SuperCable was removed from the well.

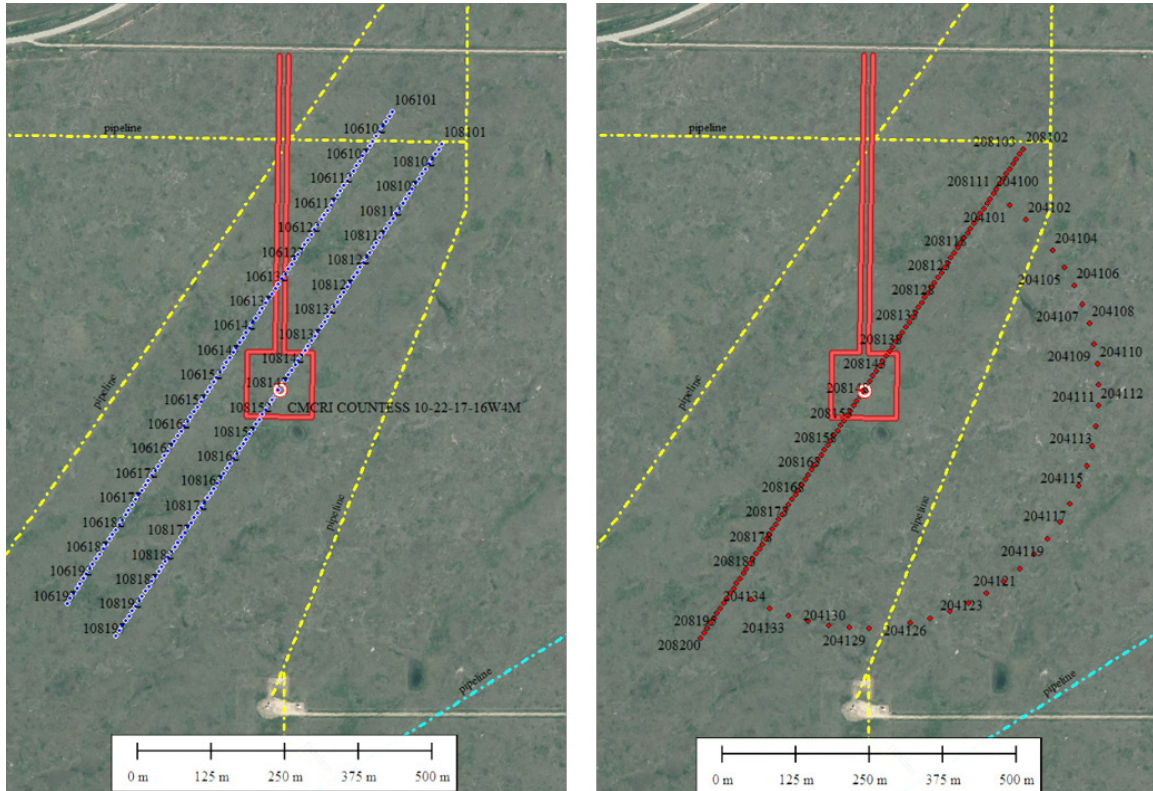


Figure 1. Map of survey area. Receiver lines 106 and 108 (left; blue dots) and Source lines 208 and 204 (right; red dots). Buried pipelines are plotted as yellow/cyan dash-dot lines. The access road and well pad are shown as solid red lines, and the well location is a red bulls-eye. North is up. Background photo courtesy of Newell County, Alberta.

BOREHOLE RESULTS

Well logs and synthetic seismograms

P-P (Figure 2) and P-S (Figure 3) synthetic seismograms were calculated from well log data. The LAS file used contained DT4P, DT4S and VPVS, however, DT4S is not continuous. Therefore, a shear sonic log was created by multiplying DT4P and VPVS. The density log (rho) was calculated in Syngram using Gardner's relationship. Reflectivity was convolved with a 10-200 Hz Vibroseis wavelet.

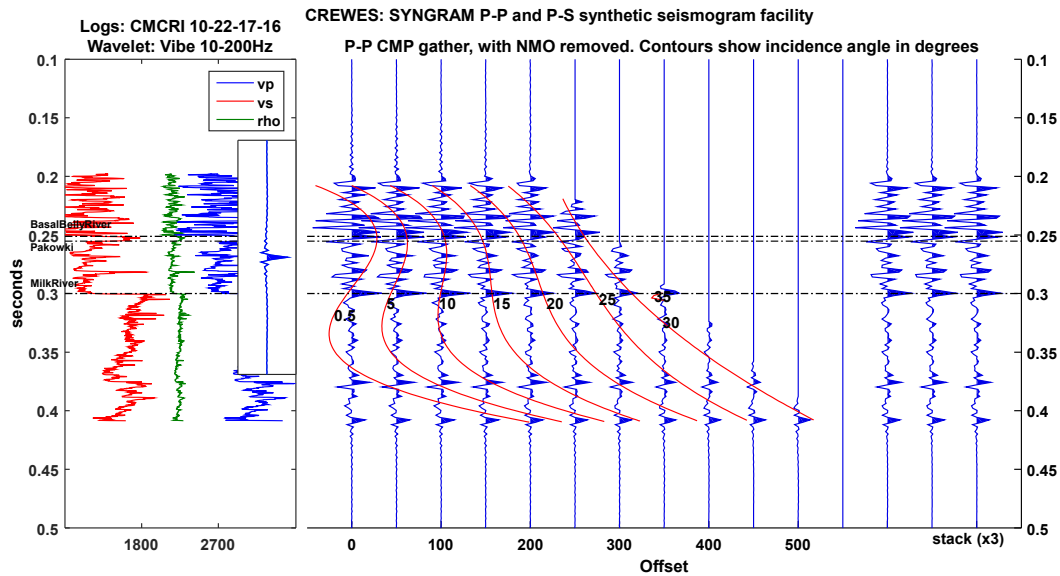


Figure 2. P-P synthetic seismogram.

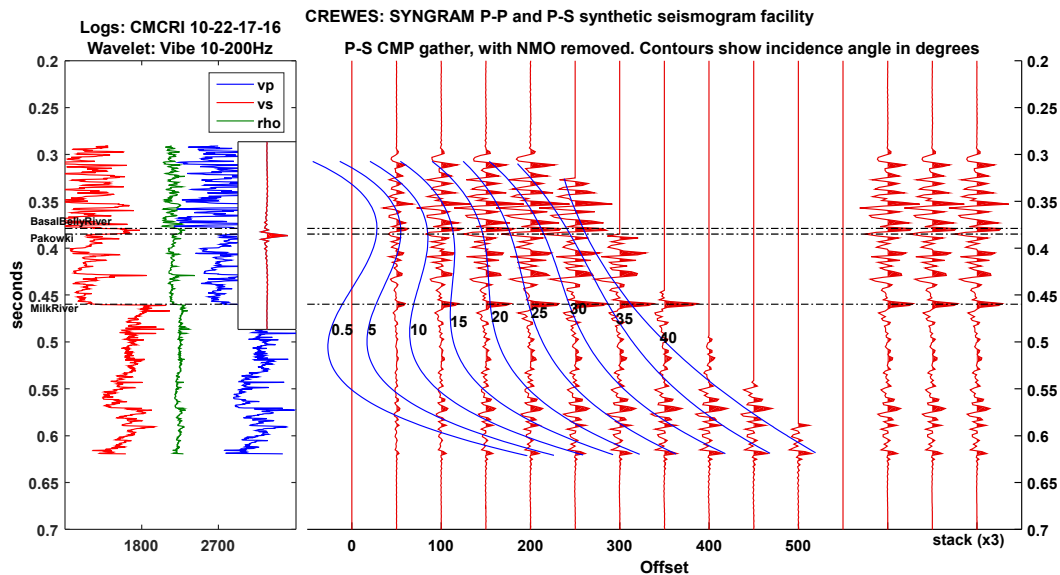


Figure 3. P-S synthetic seismogram.

Velocity analysis and characterization of anisotropy

After cross-correlating a synthetic sweep waveform and raw recordings, we automatically pick the first arrival from the peak of the amplitude envelope of the cross correlation function. Figure 4 shows the travel-time variation as a function of offset for the receiver at 406 m depth and shots along the NE-SW line (208). The data illuminate a high degree of symmetry about zero offset, suggesting that the subsurface strata are almost horizontally layered. We can further study the VTI anisotropic parameters.

The internal velocity is calculated from the derivative of depth with travel time using data of the two near offset shots (208-153, 208-149). The internal velocities from data of different sweep and different shots generally agree with each other and increase with depth from ~ 2.5 km/s at shallow depth to ~ 3 km/s at the bottom of the model (Figure 5). Figure 6 displays the azimuthal variation of the travel time obtained from data of the shots along the semi-circle line (204). We can see that the amplitude of azimuthal variation of the travel time is not very big; just several milliseconds. The fast wave propagation direction (with minimal travel time) coincides with the direction of the NE-SW line and generally follows the orientation of regional maximum horizontal compressional stress. This indicates the existence of weak HTI anisotropy likely due to fractures caused by the regional stress field.

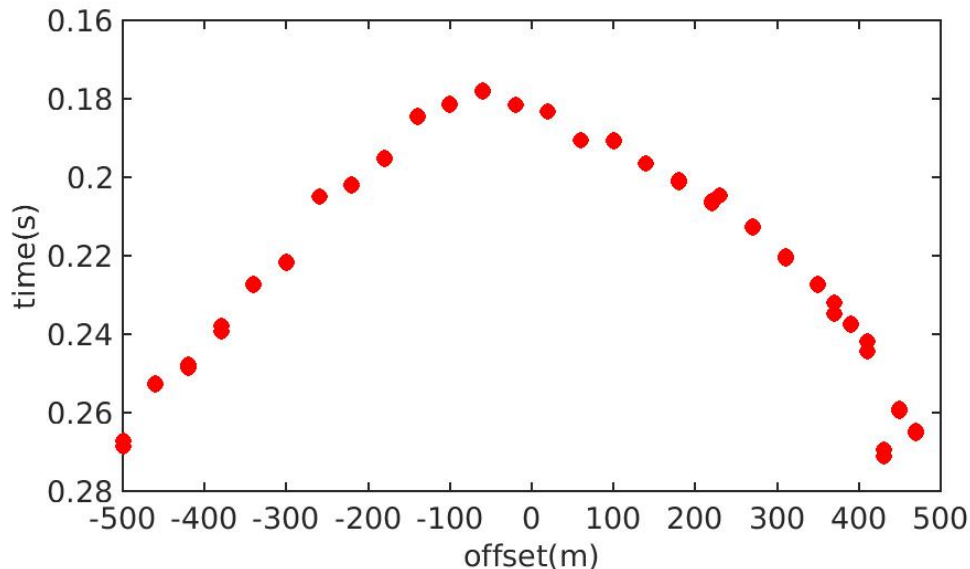


Figure 4. The variation of travel times (red dots) with offset for the receiver at 406 m depth and shots along the NE-SW line (208). Positive offsets indicate shots northeast of the well.

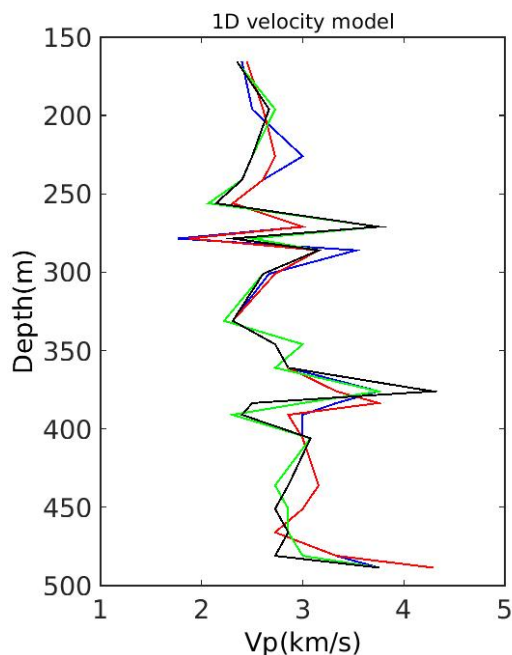


Figure 5. The 1D internal velocity models calculated from the derivative of depth with travel time using data from two near offset shots (208-153, 208-149). The offsets are ~20 m. Blue line is obtained from recordings of sweep 1 at 208-153, red line is from sweep 2 at 208-153, green line is from sweep 1 at 208-149, black line is from sweep 2 at 208-149.

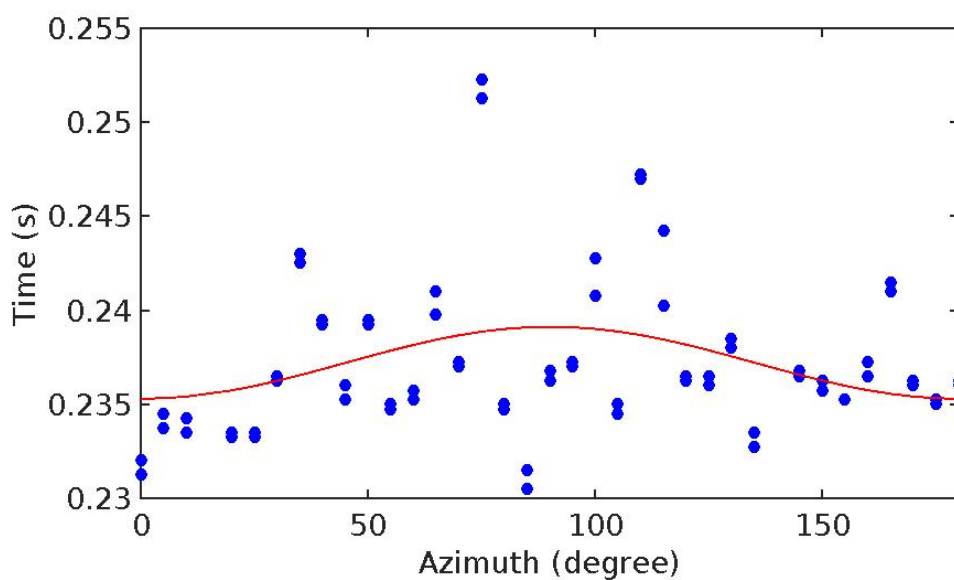


Figure 6. The variation of travel times (blue dots) with azimuth for the receiver at 383.5 m depth and shots along the semi-circle line (204). The azimuth used here is the angle between the NE-SW line and the line connecting the well and the shot. The red line is the fit to 2PSI azimuthal variation of travel times.

VSP gathers and wavefield separation

Twenty-second shot gathers were created from five-second ESG field records (Appendix B). As there are two source gathers for each VP, these were vertically stacked and correlated. The well is vertical, but we do not know how the 3C geophones were oriented within the well. Therefore, a maximum power two-component rotation was applied to rotate the horizontal components to radial and transvers components. Figure 7 shows the resulting rotation angles are within ± 10 degrees for the deep and middle tool levels. The shallowest tool level shows some large variations in rotation angle when the Vibe is closest to the well.

This method will maximize trace amplitudes on the radial component, but the end result may be normal or reverse polarity. This was followed by trace kills and polarity reversals. Finally an automatic envelope correction (AEC) was applied for display purposes. Figure 8 shows the VSP vertical and radial component gathers for VP 208149, and Figure 9 shows the corresponding amplitude spectra.

Figure 10 show the vertical component up-going wavefield after attenuation of the down-going wavefield (left), and after flattening PP-reflections based on doubling the first-break picks. We believe that P-P reflections exist in this data, but it going to require more careful processing than has been done to date to bring them out.

Both the vertical and the radial gathers contain a strong event that may be a down-going P-S conversion, followed by an up-going S-wave (Figure 8, Figure 10).

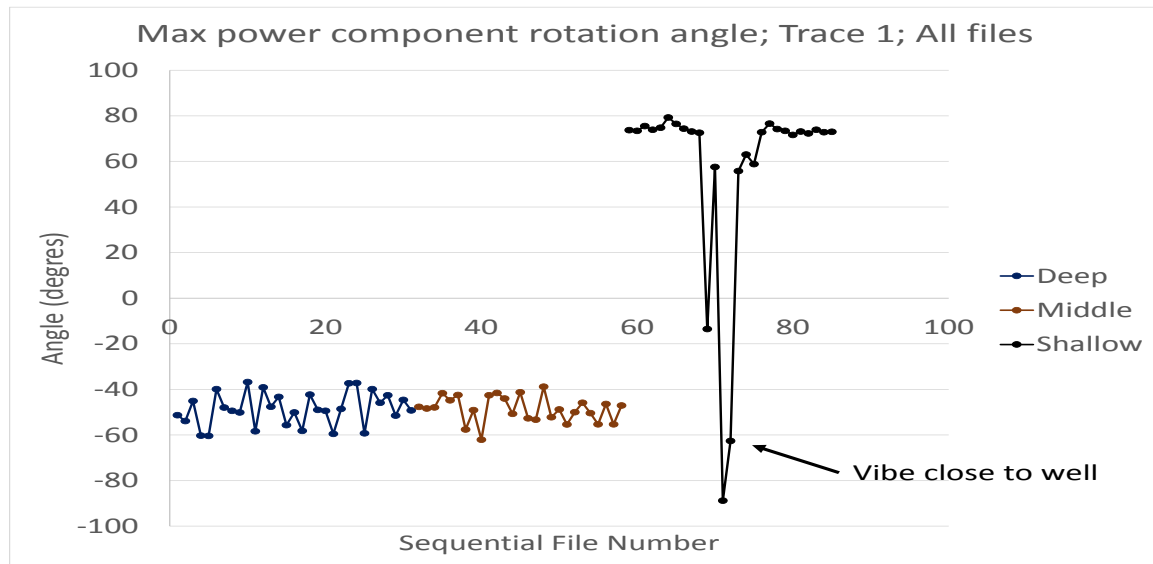


Figure 7. Component rotation angles for trace 1 (shallowest receiver in cable) for all vibe points, sorted by the three tool levels.

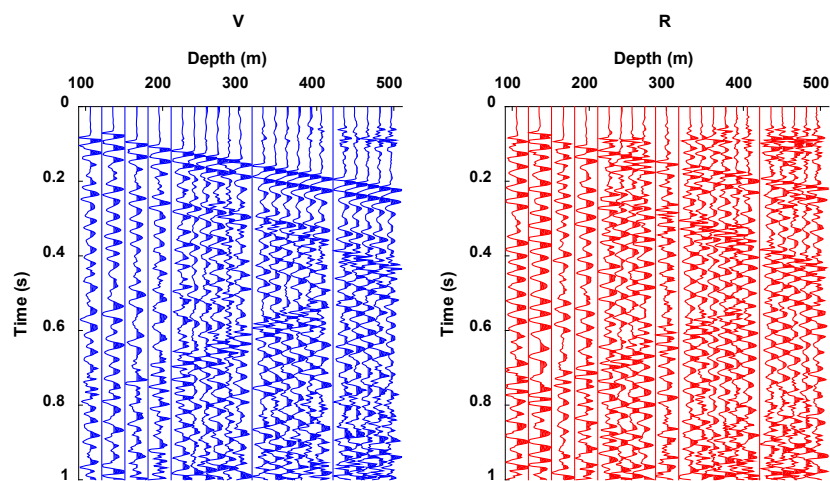


Figure 8. Sample P-P and P-S correlated source gathers for VP 208149.

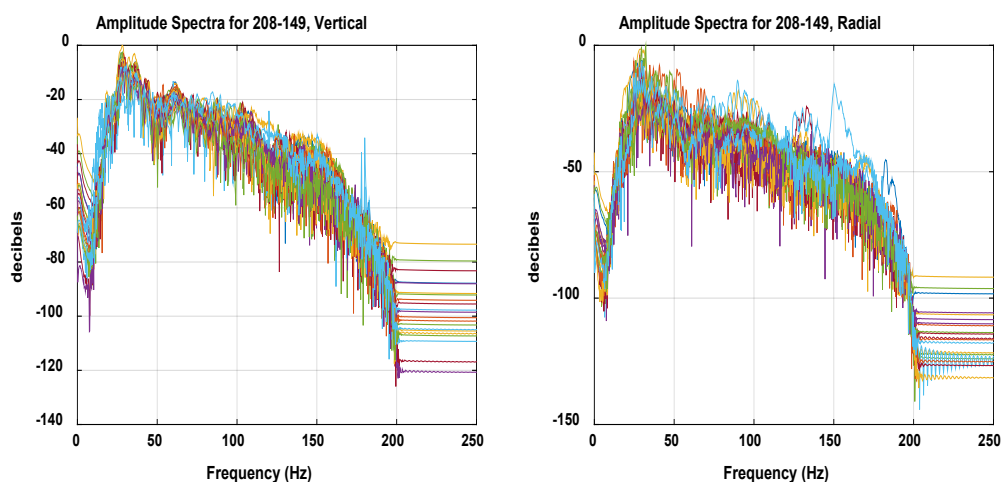


Figure 9. Amplitude spectra for VP 208149 (Figure 8).

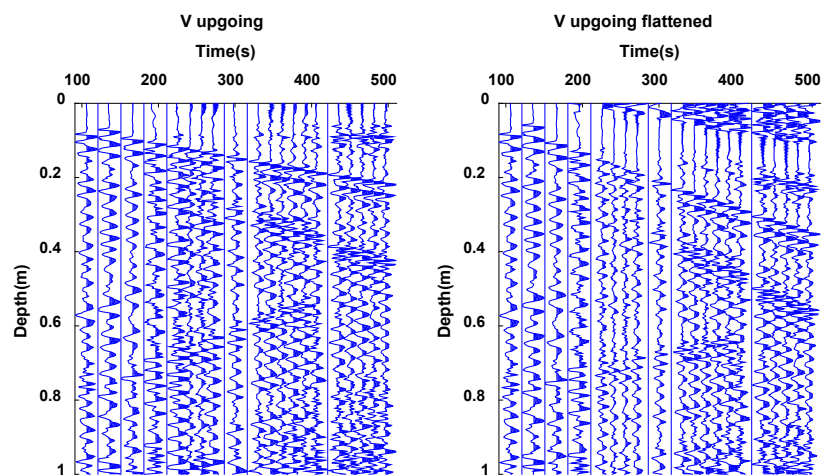


Figure 10. Vertical component up-going wave-field before (left) and after flattening P-P reflections. They're in there. We think.

SURFACE RESULTS

Testing m-sequences as Vibroseis pilots

We conducted field measurements at the Brooks Test Site in May 2015 to test the idea of driving a land vibrator with filtered maximal length sequence (m-sequence) pilots. Using the CREWES IVI EnviroVibe vibrator as the source, we recorded data along two parallel receiver lines 1000 m long with vertical geophones spaced every 10 m. For pilot signals, we used two sets of m-sequence pilots: a pure m-sequence set, and a filtered m-sequence set. Each set has four members. The pure m-sequences are characterized by step-function-like transitions between two values -1 and 1. The pure-sequences were modified by an Ormsby bandpass filter with corners at [5-10-200-250] Hz. The m-sequence pilots were all 16.376 seconds long.

At selected shot points close to Receiver Line 1, we recorded data sampled at 1 ms using each of four pure m-sequences or filtered m-sequences as the pilot driving the EnviroVibe. For comparison purposes, we also recorded data using a standard linear sweep pilot (10 to 120 Hz swept over 16 seconds with 500 ms end tapers). In all cases, listening time was 4 seconds, and in all cases we recorded both correlated and uncorrelated data as well as the signals from accelerometers mounted on the base plate and reaction mass of the vibrator. It was hoped that these accelerometer signals would provide clues as to how the hydraulically-powered vibrator reacts to the sharp/smooth transitions that are characteristic of pure and filtered m-sequences. However, issues were discovered with the linear sweep accelerometer data (Appendix A), and it is likely the m-sequence sweeps were also affected. The Brooks m-sequence tests are a continuation of similar tests using the EnviroVibe conducted in October 2013 at the Rothney test site (Wong et al., 2013).

At the present time, we have not processed or analyzed the Brooks m-sequence field data in detail.

Figure 11 shows wavelets obtained by auto-correlating TREF auxiliary traces from the Aries recorder for an unfiltered m-sequence, a bandpass filtered m-sequence and our standard 10-200 Hz linear sweep. The unfiltered m-sequence would normally be preferred due to absence of side lobes. Pure m-sequences are used to estimate the impulse response of linear systems (among many other uses). The fact that the EnviroVibe generates multiples (which are considered to be artifacts; Figure 12) in seismograms when driven by pure m-sequences means that the EnviroVibe is not a perfectly linear system, especially at high frequencies since it cannot respond accurately to the step-function-like transitions characteristic of pure m-sequences. Bandpass filtering the m-sequence before using it as a sweep introduces side-lobes in the wavelet, although smaller ones than seen for a linear sweep (Figure 11). It also reduces the prominence of the multiples in the recorded data (Figure 13). Figure 14 shows the source gather acquired with a linear sweep for comparison, and Figures 15-17 show the corresponding amplitude spectra. It is difficult to see at this scale, but the amplitude spectra for the m-sequence gather contains more energy above 250 Hz than the amplitude spectra for the filtered m-sequence gather (Figures 15 and 16).

Examination of these preliminary results indicates that the pure m-sequences and the particular filtering applied are not well suited for the EnviroVibe and its Pelton controller. It appears that the pure and currently filtered TREF pilots probably should not contain any energy above 125 Hz. In addition, we have not yet succeeded in ascertaining how the many settings available in the Pelton controller should be set in order for the hydraulics and position controls to best allow the ground force signals to closely follow the m-sequence TREF signal (for example: Should the phase lock be disabled? Can we prevent the controller from “learning”, which causes the ground force to grow with repeated sweeps?).

We note that Wong and Langton (2014, 2015) have reported very promising results from other field tests of m-sequence Vibroseis pilots.

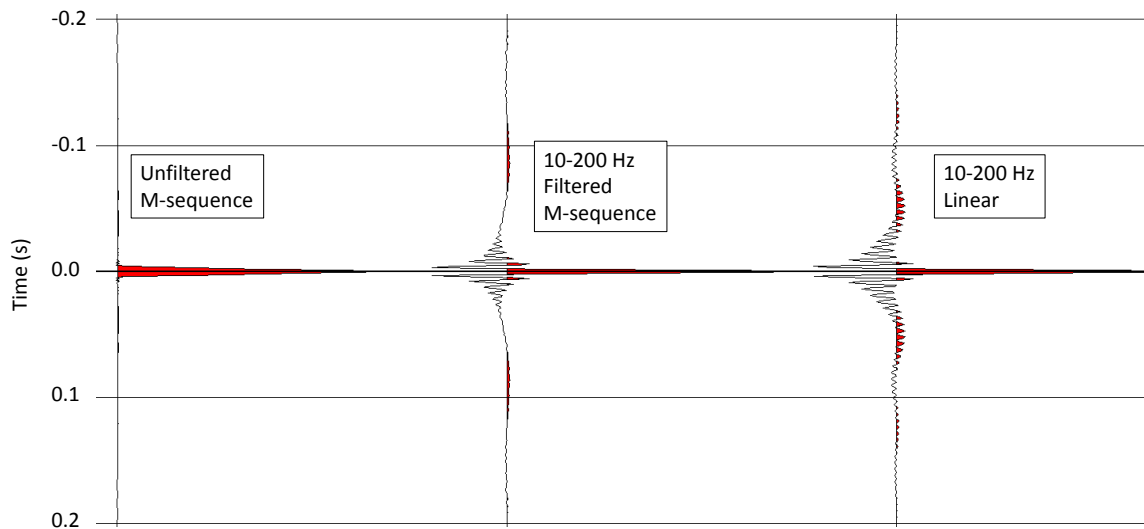


Figure 11. Examples of auto-correlated sweeps.

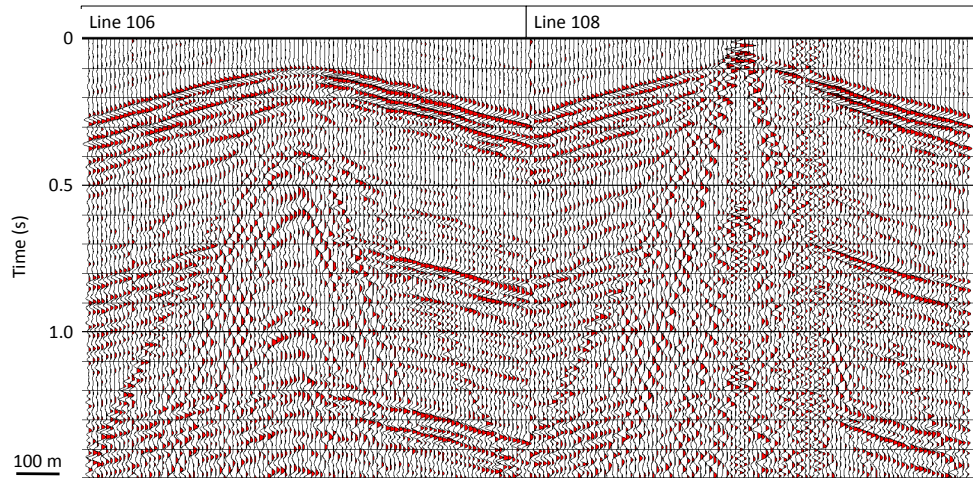


Figure 12. VP 208149 acquired using an m-sequence sweep. Bandpass and AGC for display.

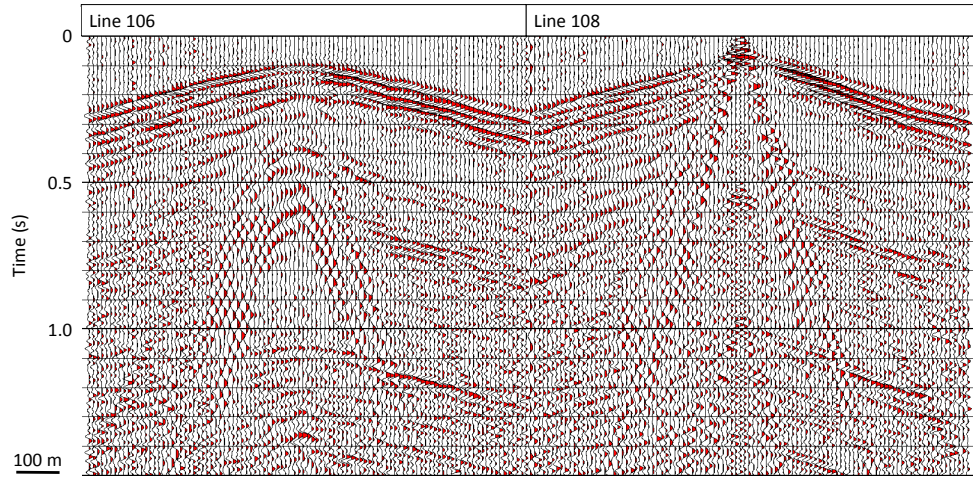


Figure 13. VP 208149 acquired using a 10-200 Hz bandpass filtered m-sequence sweep. Bandpass and AGC for display.

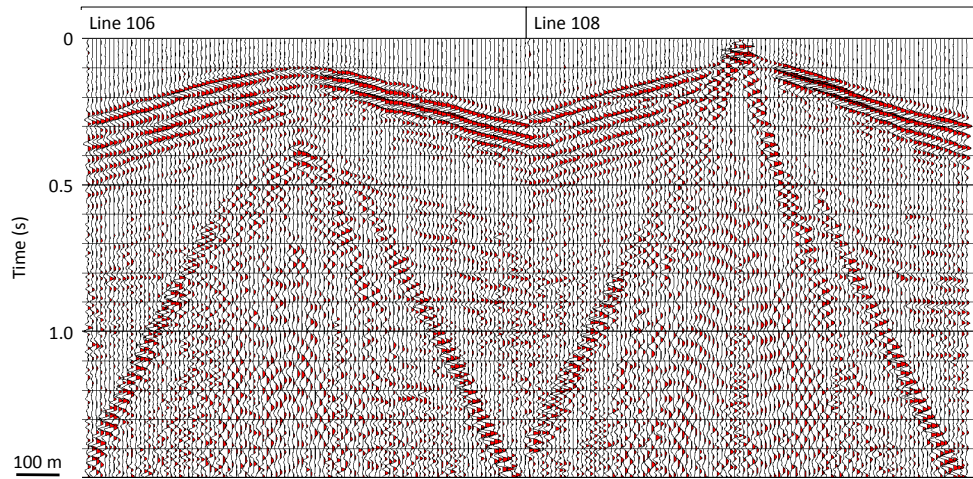


Figure 14. VP 208149 acquired using a linear 10-200 Hz sweep. Bandpass and AGC for display.

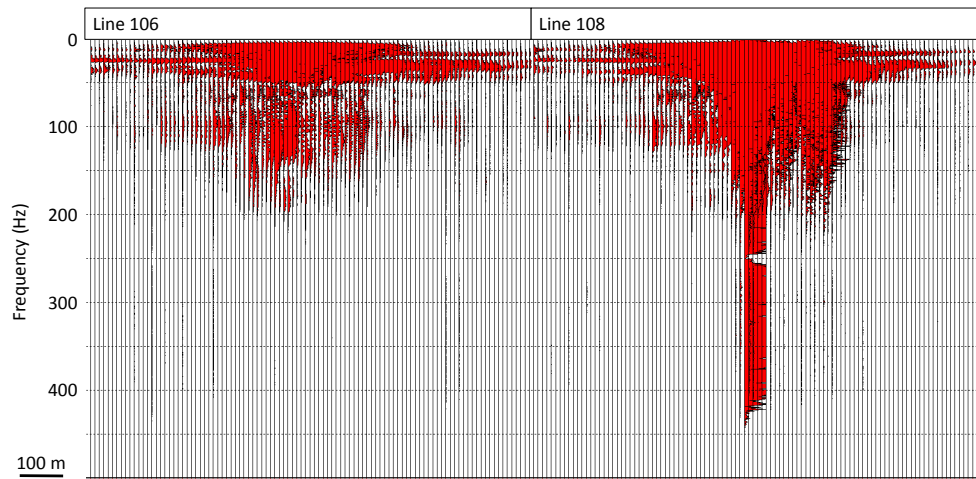


Figure 15. Amplitude spectra for VP 208149 (Figure 12) acquired using an m-sequence sweep.

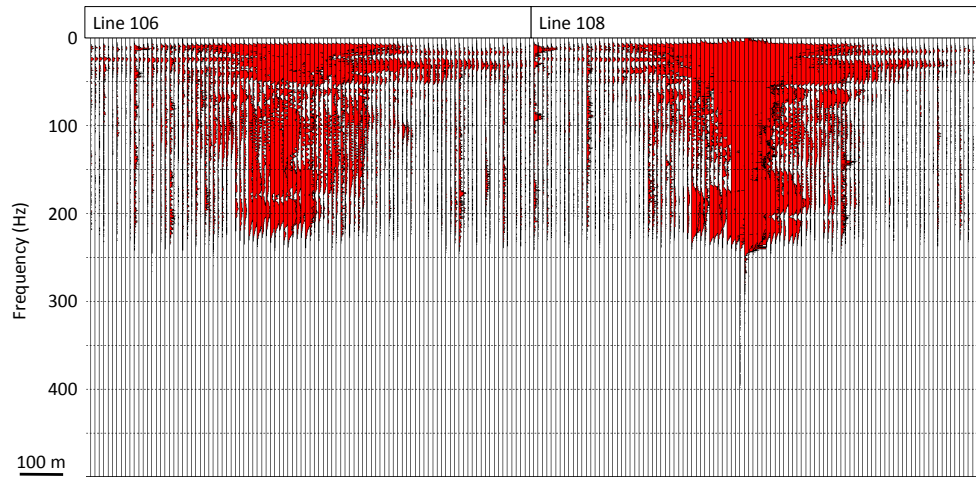


Figure 16. Amplitude spectra for VP 208149 (Figure 13) acquired using a 10-200 Hz bandpass filtered m-sequence sweep.

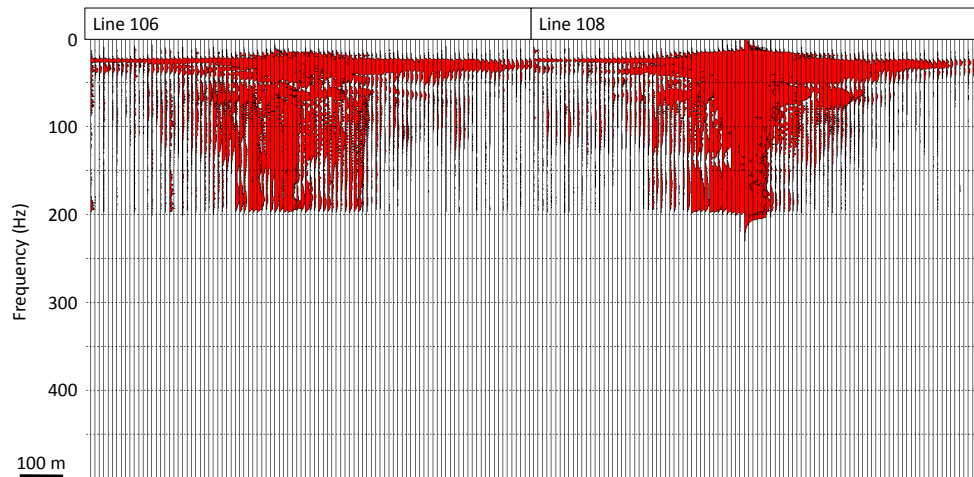


Figure 17. Amplitude spectra for VP 208149 (Figure 14) acquired using a linear 10-200 Hz sweep.

Processing of receiver line 108, Aries and Hawk

Receiver line 108 had 101 single-component SM-24 geophones spaced at 10 m (recorded with an Aries SMPL), as well as 31 three-component SM-7 geophones spaced at 30 m (recorded with Hawk nodes).

Vibe points were repeated for the ascending VSP tool and were also recorded by the surface receivers. When a VP was occupied multiple times, we selected the best by visual inspection of the source gathers.

Figure 18 shows a comparison of the same receiver gather recorded by the Aries and the Hawk systems. An AGC has been applied for display. Both datasets were processed the same way. Processing included refraction statics, air blast attenuation, spike and noise burst edit, surface wave noise attenuation, and Gabor deconvolution. Figure 19 shows the same two receiver gathers as in Figure 18 after processing.

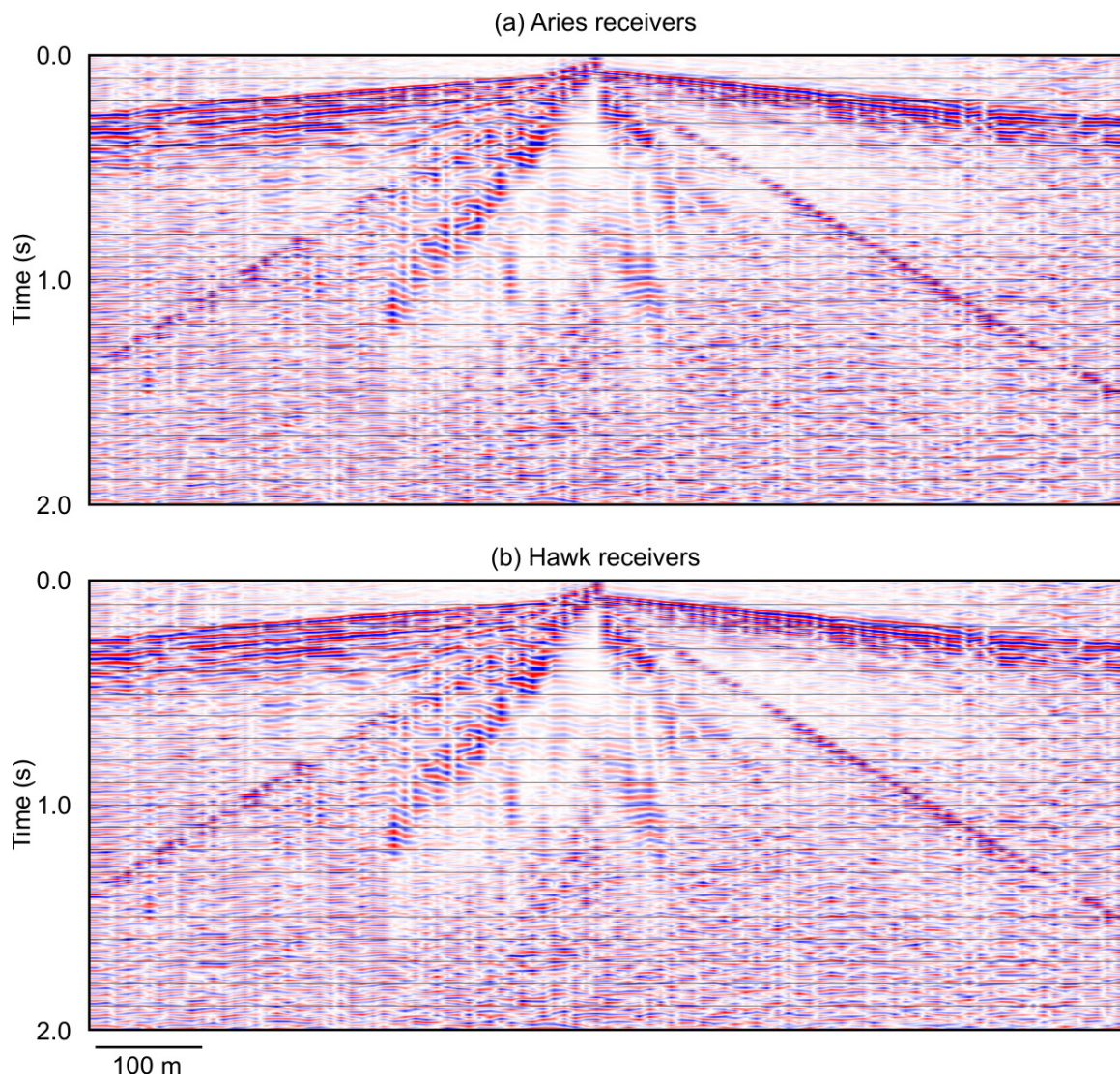


Figure 18. Field receiver gathers showing a comparison of data recorded by the (a) Aries and (b) Hawk systems. The gathers are located at the same surface station and contain the same shots.

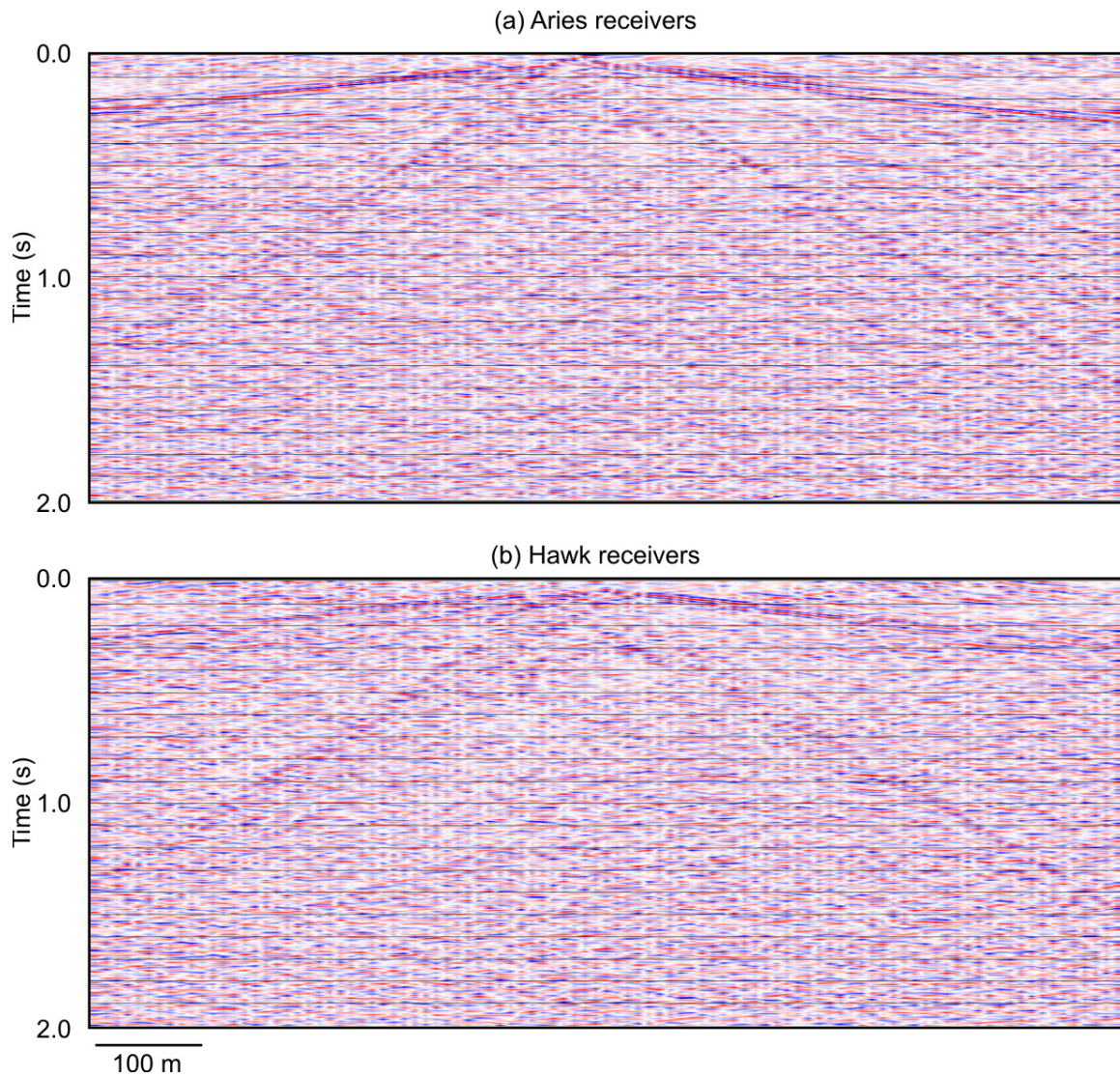


Figure 19. Processed receiver gathers.

We post-stack migrated the data using a finite difference migration and applied a bandpass filter of 10-15-80-90 Hz. The migrated data are shown in Figure 20, which also shows for comparison an arbitrary line extracted from the 2014 3D survey coinciding with the 2015 2D line. The strong event at about 0.25 s corresponds to the Basal Belly River sandstone, which is the primary CO₂ injection target at this site.

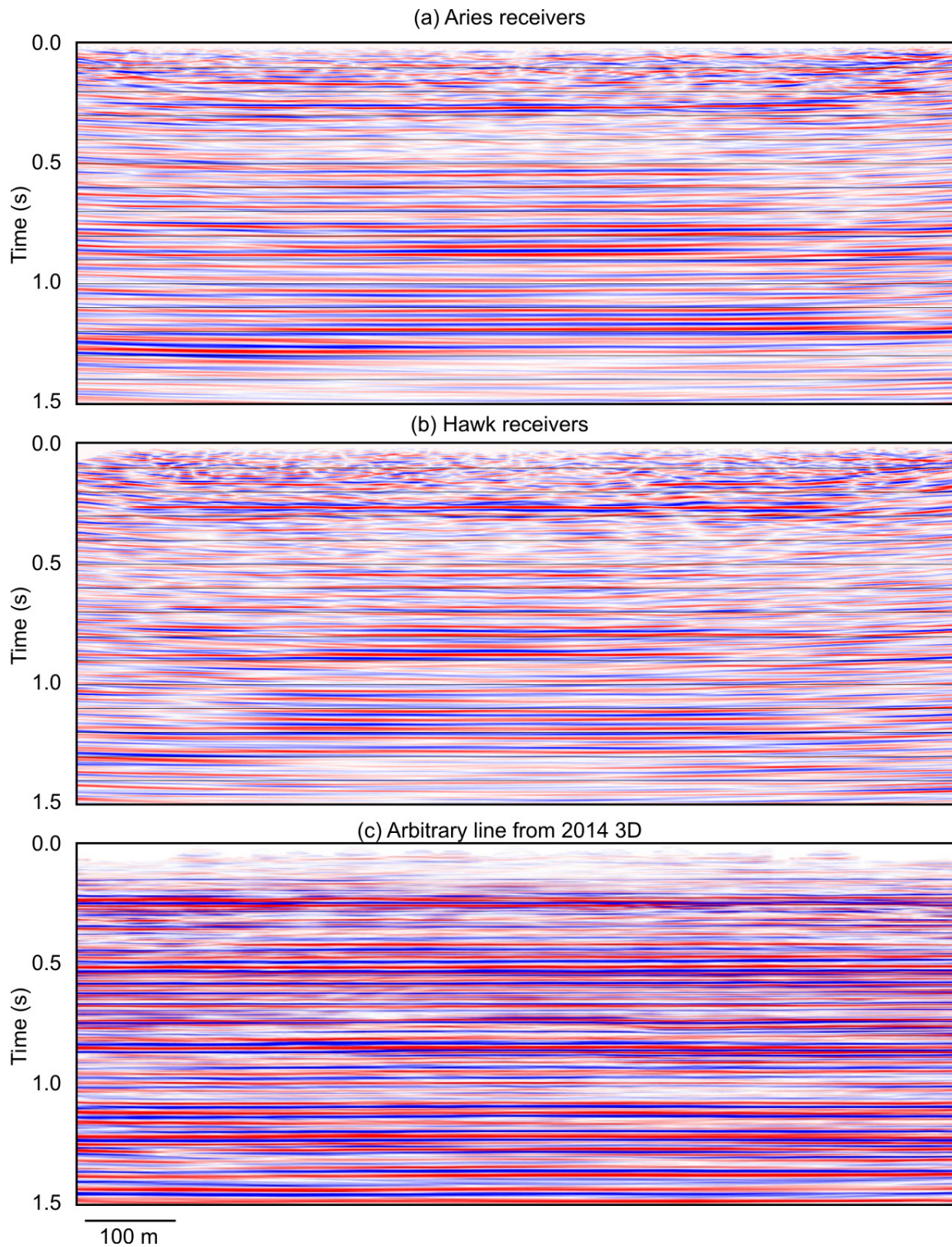


Figure 20. Post-stack migrated lines. (a) and (b) are the Aries and Hawk data, respectively, and (c) is an arbitrary line extracted from the 2014 3D corresponding to the location of the 2015 2D line.

We started to process the converted-wave data. The inline (H1) and crossline (H2) components were rotated into radial and transverse components based upon the H1 element being oriented magnetic north. Figure 21 shows a radial receiver gather before and after processing. We choose to display a receiver gather rather than a shot gather because there were only 31 3C receivers but 97 shots. The processing includes true amplitude recovery, elevation and shot statics, air blast attenuation, surface wave noise attenuation and Gabor deconvolution.

A commonly used method to determine PS receiver statics when reflectors are essentially flat is to apply NMO to receiver gathers, stack the gathers and pick a reflector to flatten by static shifts. These calculated shifts are the receiver statics. We created a PS stacking velocity file from the PP stacking velocities and V_p/V_s of 2.2. NMO was applied to the receiver gathers and the gathers were stacked. To our disappointment no clear continuous reflectors appeared on the receiver stack (Figure 22), although there are some events at around 0.55 s that are assumed to be PS reflections. We were unable to estimate receiver statics by this method and so have, thus far, not proceeded with the converted-wave processing.

We know that good PS data can be obtained at this site (Isaac and Lawton, 2015). The 2015 VSP was acquired at the same time of year and with similar ground and weather conditions as the 2014 3C-3D.

Differences between the surveys include decreased source effort for the VSP, decreased receiver effort, restricted azimuthal coverage, and the possibility that the Vibe was not actually starting to sweep at 10 Hz (Appendix A).

The 2014 3D had two simultaneous EnviroVibes doing two 10-150 Hz over 16s sweeps per vibe point at a 10 m spacing (Lawton et al., 2014), while the 2015 VSP had a single EnviroVibe doing two 10-200 Hz sweeps over 16 s.

While the receiver lines in the 3D were also 1 km long, they had 3C geophones at a 10 m spacing instead of a 30 m spacing. It is possible that the sparse receiver spacing of 30 m was insufficient for recording converted waves.

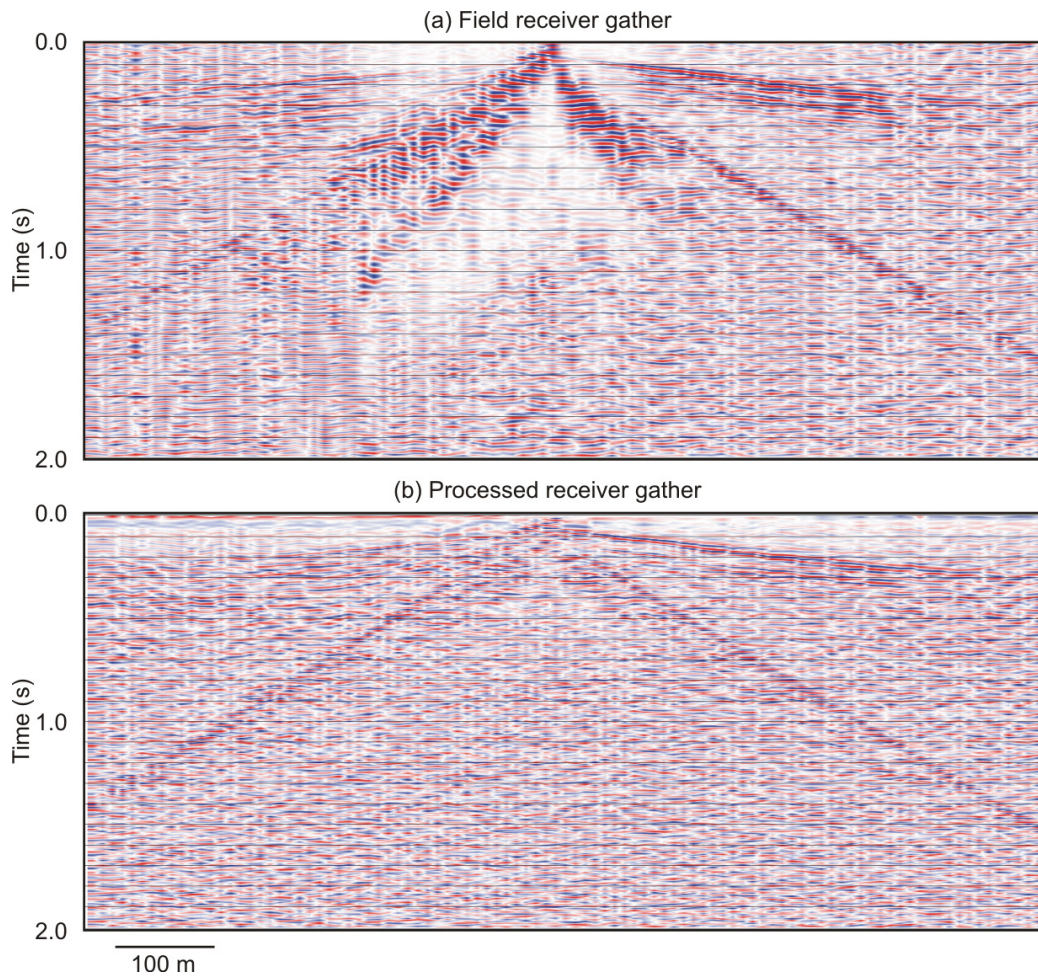


Figure 21. A field and processed receiver gather of the P-S data.

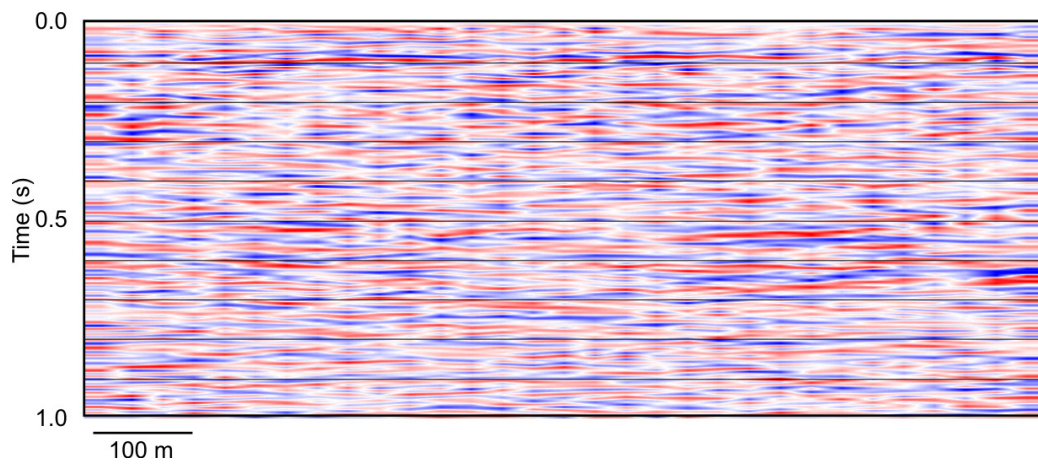


Figure 22. Stacked receiver gathers. No continuous P-S events are observed.

DISCUSSION AND FUTURE WORK

A variety of seismic work was successfully completed at the Containment and Monitoring Institute (CaMI) Field Research Station (FRS) in May of 2015. Over the course of two days data were acquired for a variety of experiments, including a walk-away 3C VSP, data for a velocity tomography study, 1C-2D and 3C-2D surface seismic, and m-sequence sweep tests. This report has shown examples of field data and issues with said data, as well as preliminary processing results.

Future work includes:

- Attempting to finalize processing of the radial component of the 3C-2D.
- Processing the near-zero-offset vertical and radial components of the VSP to corridor stacks.
- Processing the walk-away VSP data – perhaps reflections will become more clear with stacking.
- Processing the m-sequence source gathers to a migrated stack
 - Simulate multiple Vibes simultaneously running different m-sequence sweeps, and seeing how successfully the source gathers can be separated
 - Attenuating (or using) source-generated m-sequence multiples.
- Interpretation.

ACKNOWLEDGEMENTS

The authors thank the sponsors of CREWES and the Microseismic Industry Consortium, and CMC Research Institutes Inc. for access to the CaMI field research sites. This work was funded by CREWES and Microseismic Industry Consortium industrial sponsors, CMC, and NSERC (Natural Science and Engineering Research Council of Canada) through Collaborative Research and Development grants. We would also like to thank ESG for field support, as well as Halliburton (Landmark Graphics) and Schlumberger for providing donated software.

REFERENCES

- Isaac, J. H. and Lawton, D.C., 2015, 3D3C seismic data at the Brooks experimental CO₂ injection site: CREWES Research Report, **27**, 31.
- Lawton, D. C., Bertram, M. B., Bertram, K. L., Hall, K. W., and Isaac, J. H., 2014, A 3C-3D seismic survey at a new field research station near Brooks, Alberta: CREWES Research Report, **26**, 48.
- Wong, J., Bertram, M., Bertram, K., Gallant, E., and Hall, K., 2013, Controlling a land vibrator with m-sequences: a field test: CREWES Research Report, **25**, 80.
- Wong, J., and Langton, D., 2014, Simultaneous multi-source acquisition using m-sequences: CREWES Research Report, **26**, 77.
- Wong, J., and Langton, D., 2015, Field and numerical investigation of filtered m-sequence pilots for Vibroseis acquisition: CREWES Research Report, **27**, 73.

APPENDIX A

A Geode recorder was present in the cab of the EnviroVibe to record auxiliary traces, including data from the Vibe's ground force accelerometer, directly from the Pelton decoder.

After the survey was completed, it was noticed that while the sweep stored as the true reference (TREF) is unchanged, the other auxiliary traces differ after a series of bad sweeps and a decoder reset in the Vibe (Table A.1, Figure A.1). The sweep start time is delayed by approximately two seconds from time-zero, while the end time remains the same (orange/black lines, Figure A.1). The uncorrelated Aries shot gathers contain two auxiliary traces, Time Break and TREF. Equivalent Aries shot gathers show no change in these traces before and after the Vibe decoder reset.

An examination of the amplitude spectra of the Geode auxiliary traces (Figure A.2) shows that the shortened and delayed sweeps are missing frequencies between 10 and ~25 Hz. However, uncorrelated data traces from the Aries recorder for the same Vibe Points show no equivalent changes in amplitude spectra. However, the amplitude starts to drop off at about 25 Hz both before and after the decoder reset (Figure A.3).

So we do not know what happened. Anecdotal evidence from the Vibe operator suggests that the delayed start was observed in the field, but was thought to be less than 0.5 s rather than 2.0 s. Assuming we can trust the accelerometer data, the fact that we do not see 10 Hz data in the Aries shot gathers may mean that we were not generating these frequencies with the Vibe, or this area at this time was not conducive to acquiring frequencies below 25 Hz anyway.

All correlated data shown in this report were correlated using TREF. We would not recommend using the Geode data without careful thought and further analysis.

Table A.1.

| Geode File number | Comment (observation) | Aries File number | Comment | Station |
|-------------------|-----------------------|-------------------|-----------------------|---------|
| 346 | OK | 192 | 2 nd sweep | 204102 |
| 350 | OK | 194 | 1 st sweep | 208112 |
| 351 | BAD | Null | None | None |
| 352 | BAD | Null | None | None |
| 353 | BAD | 197 | 1 st sweep | 208114 |
| 354 | BAD | 200 | 1 st sweep | 208116 |
| 355 | DELAYED START | 201 | 2 nd sweep | 208116 |
| 356 | DELAYED START | 203 | 1 st sweep | 208120 |
| 357 | DELAYED START | 204 | 2 nd sweep | 208120 |
| 358 | DELAYED START | 209 | 1 st sweep | 208128 |

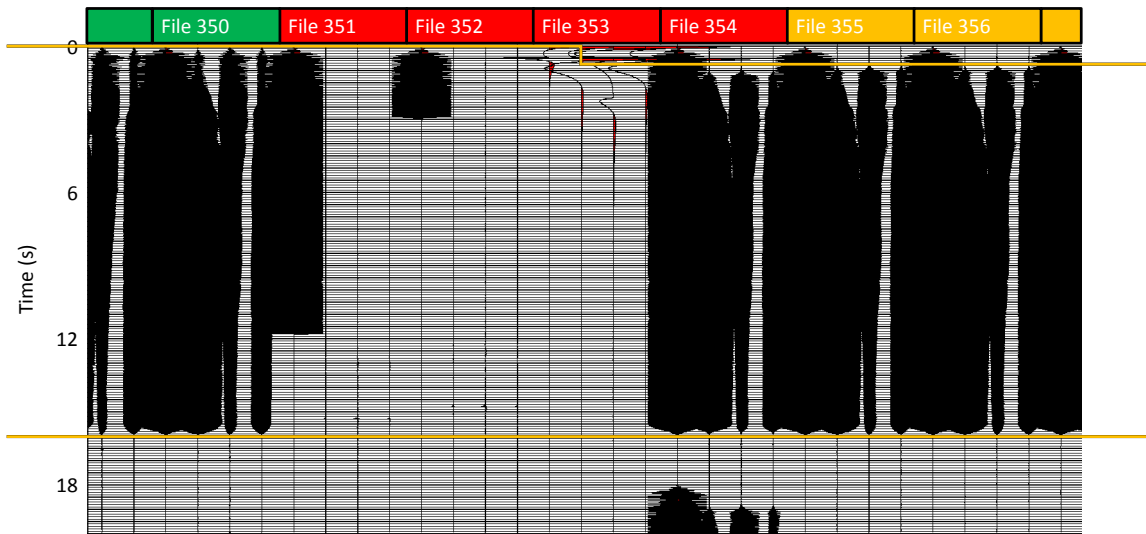


Figure A.1. Auxiliary traces recorded on Geode from Pelton decoder before and after some bad sweeps and a decoder reset. In each file Aux 1 = TREF, Aux 2 = baseplate accelerometer, Aux 3 = mass accelerometer, Aux 4 = ground force (derived from Aux 2 and 3).

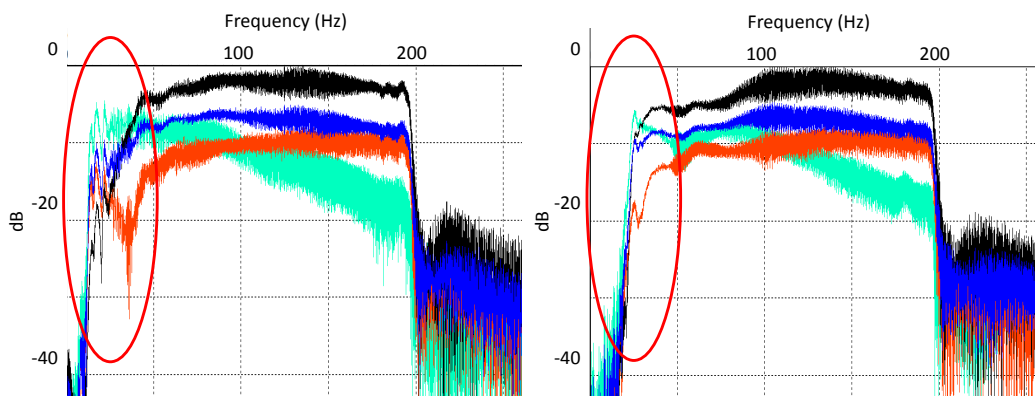


Figure A.2. Amplitude spectra excluding TREF for Geode files 350 (left; before decoder reset) and 358 (right; after decoder reset). Dark blue is average of all three aux traces.

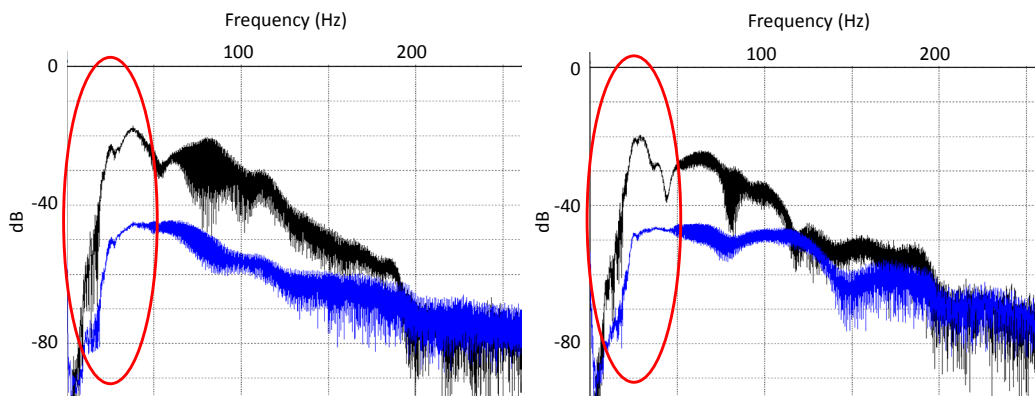


Figure A.3. Amplitude spectra for uncorrelated Aries data traces for Aries files 194 (left; Same VP as Geode file 350; Before decoder reset) and 209 (Right; Same VP as Geode file 358; After decoder reset). Black is trace 10 m from Vibe. Blue is average of all data traces.

APPENDIX B

ESG Paladin recorders provide five second SEG-Y files where the GPS time of the first sample is encoded in the directory structure and filename. The last sample of a SEG-Y file has the same time as the first sample of the next file.

The Verif-i unit in our recording truck places the GPS time of shot in the Aries observer's notes as a Synctime column. For this survey, the Verif-i Synctime was six hours ahead of the ESG time due to using a different time zone (Figure B.1).

A Matlab script was written to vertically concatenate the 5 second files containing time-zero plus twenty seconds and truncate to twenty second records. Note that the required ESG SEG-Y files can be in different hour or even different day and hour folders.

Traces recorded at all three tool levels were then merged to create a single shot gather with a 15 m trace spacing (Table B.1).

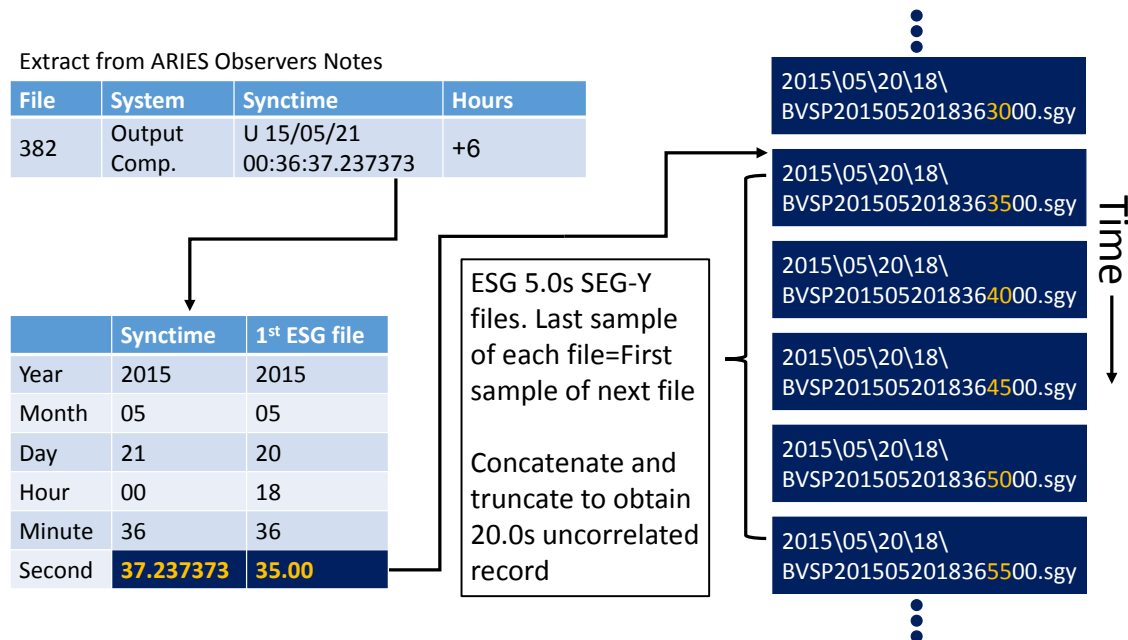


Figure B.1. Converting Verif-i Synctime in Aries observer's notes into a 20.0 s uncorrelated shot gather from ESG 5.0 s SEG-Y files.

Table B.1. Trace merge to generate a single shot gather with 15 m trace spacing from deployment 1 (deep), 2 (middle) and 3 (shallow).

| deployment | level | outrc | trc_dep3 | trc_dep2 | trc_dep1 | depth (m) | interval (m) |
|------------|-------|-------|----------|----------|----------|-----------|--------------|
| 3 | 3 | 1 | 1 | 0 | 0 | 106 | |
| 0 | 0 | 2 | 0 | 0 | 0 | 121 | 15 |
| 3 | 4 | 3 | 2 | 0 | 0 | 136 | 15 |
| 0 | 0 | 4 | 0 | 0 | 0 | 151 | 15 |
| 3 | 5 | 5 | 3 | 0 | 0 | 166 | 15 |
| 0 | 0 | 6 | 0 | 0 | 0 | 181 | 15 |
| 3 | 6 | 7 | 4 | 0 | 0 | 196 | 15 |
| 2 | 3 | 8 | 0 | 1 | 0 | 211 | 15 |
| 3 | 7 | 9 | 5 | 0 | 0 | 226 | 15 |
| 3 | 8 | 10 | 6 | 0 | 0 | 241 | 15 |
| 3 | 9 | 11 | 7 | 0 | 0 | 256 | 15 |
| 2 | 5 | 12 | 0 | 3 | 0 | 271 | 15 |
| 3 | 12 | 13 | 10 | 0 | 0 | 286 | 15 |
| 2 | 6 | 14 | 0 | 4 | 0 | 301 | 15 |
| 1 | 3 | 15 | 0 | 0 | 1 | 316 | 15 |
| 2 | 7 | 16 | 0 | 5 | 0 | 331 | 15 |
| 2 | 8 | 17 | 0 | 6 | 0 | 346 | 15 |
| 2 | 9 | 18 | 0 | 7 | 0 | 361 | 15 |
| 1 | 5 | 19 | 0 | 0 | 3 | 376 | 15 |
| 2 | 12 | 20 | 0 | 10 | 0 | 391 | 15 |
| 1 | 6 | 21 | 0 | 0 | 4 | 406 | 15 |
| 0 | 0 | 22 | 0 | 0 | 0 | 421 | 15 |
| 1 | 7 | 23 | 0 | 0 | 5 | 436 | 15 |
| 1 | 8 | 24 | 0 | 0 | 6 | 451 | 15 |
| 1 | 9 | 25 | 0 | 0 | 7 | 466 | 15 |
| 1 | 10 | 26 | 0 | 0 | 8 | 481 | 15 |
| 1 | 12 | 27 | 0 | 0 | 10 | 496 | 15 |